Journal of Medicinal Chemistry

Article

pubs.acs.org/jmc

Peptide Half-Life Extension: Divalent, Small-Molecule Albumin Interactions Direct the Systemic Properties of Glucagon-Like Peptide 1 (GLP-1) Analogues

Esben M. Bech,[†,‡] Manuel C. Martos-Maldonado,[†] Pernille Wismann,[‡] Kasper K. Sørensen,[†] Søren Blok van Witteloostuijn,[‡] Mikkel B. Thygesen,[†] Niels Vrang,[‡] Jacob Jelsing,[‡] Søren L. Pedersen,*[,‡] and Knud J. Jensen*[,†]

[†]Department of Chemistry, University of Copenhagen, Frederiksberg 1870, Denmark

[‡]Gubra Aps, Hørsholm 2970, Denmark

Supporting Information

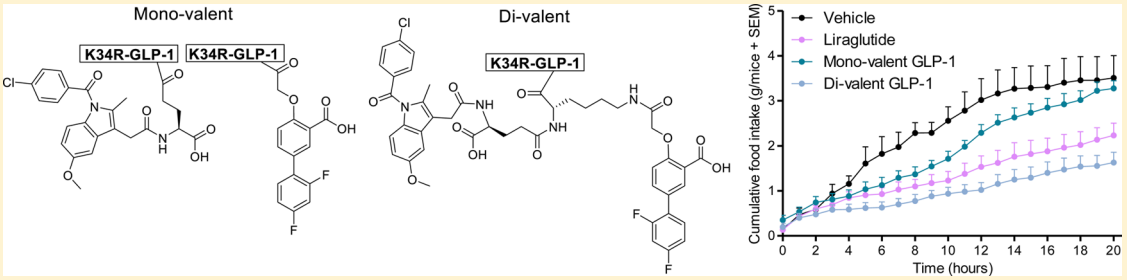

ABSTRACT: Noncovalent binding of biopharmaceuticals to human serum albumin protects against enzymatic degradation and renal clearance. Herein, we investigated the effect of mono- or divalent small-molecule albumin binders for half-life extension of peptides. For proof-of-principle, the clinically relevant glucagon-like peptide 1 (GLP-1) was functionalized with diflunisal, indomethacin, or both. In vitro, all GLP-1 analogues had subnanomolar GLP-1 receptor potency. Surface plasmon resonance revealed that both small molecules were able to confer albumin affinity to GLP-1 and indicated that affinity is increased for divalent analogues. In lean mice, the divalent GLP-1 analogues were superior to monovalent analogues with respect to control of glucose homeostasis and suppression of food intake. Importantly, divalent GLP-1 analogues showed efficacy comparable to liraglutide, an antidiabetic GLP-1 analogue that carries a long-chain fatty acid. Finally, pharmacokinetic investigations of a divalent GLP-1 analogue demonstrated a promising gain in circulatory half-life and absorption time compared to its monovalent equivalent.

INTRODUCTION

Human serum albumin (HSA) is the most abundant protein in sera, where it primarily functions as a transporter for a myriad of molecules.[1] Among the bound molecules are fatty acids, which are known to have high albumin affinities. Peptide lipidation therefore promotes albumin interactions and can be exploited to improve the pharmacokinetic properties of peptide pharmaceuticals. This strategy has been successfully applied as exemplified by liraglutide, a GLP-1 analogue, and insulin detemir, a long-acting human insulin analogue, which are blockbuster drugs within the field of diabetes. For liraglutide, lipidation extends the circulatory half-life of GLP-1 from about 1 h to approximately 13 h in humans upon subcutaneous administration.[2,3] However, lipidation is not generally applicable for peptide pharmaceuticals, as it can lead to a drastic reduction in solubility. Consequently, alternative strategies for mediating albumin interactions with enhanced HSA affinity, solubility, or additional medicinal properties continues to be attractive.[4] Herein, we addressed an alternative methodology by conjugating of small-molecule albumin binders to peptides.

Anionic aromatic small molecules generally have high affinities for albumin and can be used as alternatives to lipidation. Small-molecule drugs primarily bind two sites in albumin, namely drug site I and II. The sites are structurally dissimilar, as drug site I comprises a central area from which three subchambers protrude, while drug site II consists of a single narrow crevise.[5] Of the two, drug site I is by far larger and is even capable of binding two different small molecules simultaneously.[5] For a selection of small-molecule drugs, high affinities for drug site I or II have resulted in low in vivo efficacy compared to in vitro potency, and this has prompted the search for analogues with reduced HSA interaction.[6−9] Compared to small molecule drugs, peptides generally have higher receptor potencies, and peptides are therefore less vulnerable to efficacy lowering effects stemming from HSA bindings. Thus, conjugating small-molecule drugs with high HSA affinities to prolong peptide half-life is an interesting alternative to

Received: May 30, 2017
Published: August 3, 2017

DOI: 10.1021/acs.jmedchem.7b00787
J. Med. Chem. 2017, 60, 7434−7446

Scheme 1. Synthesis of 11: Preparation of Diflunisal for Solid-Phase Peptide Synthesis

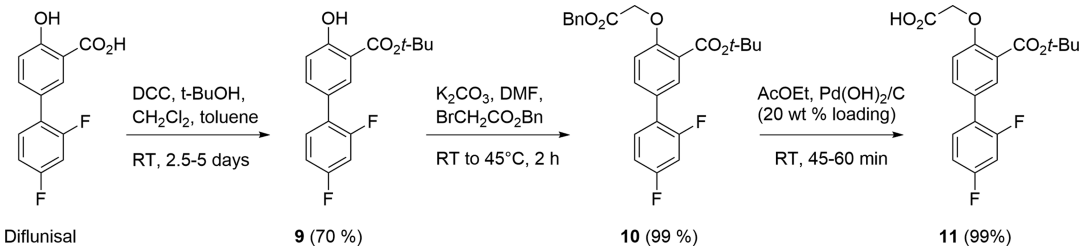

lipidation.[10−14] It has previously been demonstrated that GLP-1 conjugated to the small-molecule, monovalent albumin binder dicoumarol has a prolonged in vivo half-life in rats, as compared to liraglutide.[12]

Multivalent small-molecule albumin ligands might further enhance peptide pharmacokinetics. To our best knowledge, all examples of peptide half-life extensions using small-molecule drugs have only utilized a single albumin ligand, i.e., monovalent albumin binding. Multivalent ligands have multiple affinities (avidity) for their targets, and the avidity of a multivalent ligand can be much higher than the sum of affinities for its inherent components.[15] Consequently, we hypothesized that multivalent small molecule albumin binders would be an effective method to further extend the circulatory half-lives of peptide pharmaceuticals.

To investigate this hypothesis, we performed a series of proof-of-principle studies on peptides conjugated to one or two small-molecule albumin ligands (i.e., mono- and divalent). As a model peptide, we selected an analogue of native GLP-1 (**1**), [K34R]-GLP-1(7-37)-OH (**2**). In itself, GLP-1(7-37)-OH is a well characterized peptide hormone with short systemic half-life (1−2 min) and high clinical relevance,[16] and the K34R substitution allows for selective modifications at Lys26. Furthermore, peptide **2** is the backbone structure of liraglutide which is commonly used as a positive control and benchmark molecule in proof-of-principle studies in research on diabetes type 2. From **2**, six peptides (**3**−**8**) with albumin mono- or divalency were synthesized.

For proof-of-principle, we selected the small-molecule drugs diflunisal and indomethacin as albumin ligands because of their well-characterized, high-affinity albumin binding properties.[5,17−19] Diflunisal binds HSA with a K_D of 3 μM through both drug site I and II as well as a less well-defined site between albumin subdomain IIA and IIB.[5,6] Indomethacin binds HSA with a K_D of 0.7 μM through drug site I and a lesser site in albumin subdomain IB.[20] A noteworthy feature of indomethacin's binding to drug site I is its position in the cavity. While most drugs bind site I in the central part and/or near the entrance of the cavity, indomethacin occupies the front and lower parts.[5] This unusual position allows for the simultaneous binding of indomethacin and another small molecule to drug site I, as previously demonstrated with the two centrally binding compounds azapropazone and phenylbutazone.[5,21] As diflunisal binds drug site I exclusively at the entrance of the cavity,[5] we hypothesize that cobinding can be achieved with diflunisal and indomethacin. If this could be accomplished, peptides conjugated to both diflunisal and indomethacin should be able to bind four different sites on HSA and bind drug site I in a divalent, high-avidity fashion.

Diflunisal and indomethacin are both nonsteroidal anti-inflammatory drugs (NSAIDs) which inhibit cyclooxygenase (COX) 1 or 2.[6,22,23] We hypothesize that NSAID's conjugated to peptide hormones like GLP-1 will not generate NSAID-derived effects. COX is exclusively intracellularly located, while the GLP-1 receptors are located at the cell surface. In an elegant study from 2012, Finan and colleagues demonstrated how the conjugation of estrogen to a GLP-1 analogue abolish adverse estrogenic properties in tissues with low/no expression of the GLP-1 receptor.[24] Also, diflunisal and indomethacin are normally administered in hundreds of mg/day and with 80−100% bioavailability their pharmacologically relevant doses far exceed that of GLP-1 agonists (recommended dose of liraglutide is 0.6−1.8 mg/day).[25−27]

In the present study, we investigated divalent small-molecule albumin binders as an approach to improve peptide pharmacokinetics. For this purpose, we performed proof-of-principle studies using GLP-1 analogues conjugated to either diflunisal, indomethacin, or both.

RESULTS

Design and Synthesis of GLP-1 Analogues. To investigate multivalent small-molecule albumin binders as a methodology to enhance peptide pharmacokinetics, we conjugated diflunisal, indomethacin, or both to a GLP-1 model peptide, **2**. Both indomethacin and diflunisal contains a single carboxylic acid. This acid is highly important for diflunisal's binding to HSA.[6] In contrast, the hydroxyl group of diflunisal can be removed with little impact on HSA affinity.[6] Hence, diflunisal was modified to enable GLP-1 conjugation through its hydroxyl group (Scheme 1). The native carboxylic acid of diflunisal was protected as the *tert*-butyl ester (**9**), and subsequently the hydroxyl group was alkylated with benzyl bromoacetate by a Williamson ether synthesis (**10**).[28] Finally, the introduced benzyl ester was deprotected by palladium-catalyzed hydrogenation affording a diflunisal analogue, **11**, ready for solid-phase peptide synthesis (SPPS). A similar synthesis route, via **12**−**14**, was used to make the defluorinated analogue of diflunisal, **15** (Supporting Information, Scheme 1). Following SPPS, the *tert*-butyl group protecting the carboxyl groups of **11** and **15** was removed by acid-catalyzed hydrolysis.

Like diflunisal, the carboxylic acid of indomethacin is involved in its interaction with HSA.[5] However, a certain degree of flexibility is allowed for this carboxylic acid, as it can bind either HSA amino acid Arg218 or flip and interact with K199.[5] Hence, we hypothesized that albumin affinity would be retained when linking indomethacin to the GLP-1 analogues through the indomethacin carboxyl as long as another carboxyl group is sterically close. For this reason, indomethacin was incorporated into the GLP-1 analogues through the N^{α}-amine of a glutamic acid with a free α-carboxylic acid, a γGlu.

Five peptides, **3**−**7**, with either albumin mono- or divalency were synthesized by selective elongation of **2** at the ε-amine of Lys26 using Fmoc-based SPPS (Scheme 2). Selectivity was ensured by protection of the N-terminal α-amino group with

DOI: 10.1021/acs.jmedchem.7b00787
J. Med. Chem. 2017, 60, 7434−7446

Scheme 2. Synthesis Strategy for Creating GLP-1 Analogues Containing Small-Molecule Albumin Binders[a]

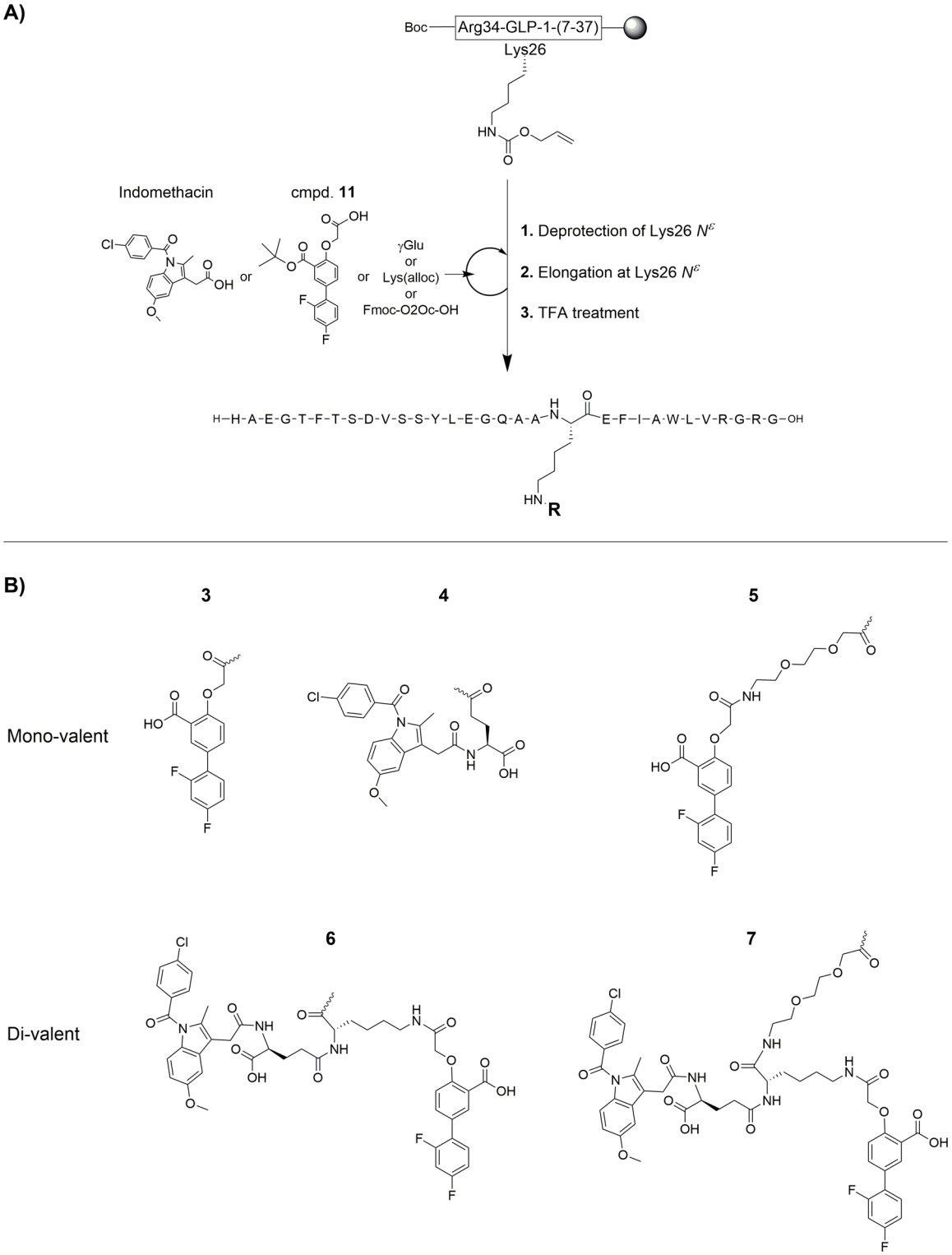

[a](A) Fully protected Boc-[K34R]-GLP-1(7-37)-OH was synthesized by Fmoc-SPPS. Next, Lys26 ε-amine was selectively deprotected and subsequently modified for HSA mono- or divalency. Finally, TFA was used to deprotect- and release GLP-1 analogues **3**–**7**. **R** denotes either of the ligands shown in (B).

the base-stable *tert*-butyloxycarbonyl (Boc) group. GLP-1 analogues **3**, **4**, and **6** were synthesized to enable comparison of mono- and divalent albumin valency, while peptides **5** and **7** contained an 8-amino-3,6-dioxaoctanoic acid (O2Oc) spacer allowing the investigation of the importance of a spacer. A sixth monovalent peptide (**8**) resembling **3** was synthesized in the same way (Supporting Information, Figure 13).

GLP-1 Receptor Potency. The novel GLP-1 analogues were applied to a GLP-1 receptor (GLP-1R) cAMP activity assay to study whether attachment of the small molecules had

DOI: 10.1021/acs.jmedchem.7b00787
J. Med. Chem. 2017, 60, 7434–7446

Table 1. in Vitro Characterization of Native GLP-1 (1) and Derivatives of the Liraglutide Backbone Peptide (2) Modified at the Side Chain of lys26[a]

compd	backbone	K27 N^{ε} modification	HSA valence	GLP-1 R EC_{50} ± SEM (nM)	apparent M_w (kD)	oligomeric state (m)	r_H ± SEM (nm)
1	GLP-1(7-36)-NH_2		none	0.044 ± 0.006			
2	[K34R]-GLP-1(7-37)-OH		none	0.023 ± 0.004	5.1	1.5	
liraglutide	[K34R]-GLP-1(7-37)-OH	-γGlu-palmitic acid	mono	0.067 ± 0.009	43.4	11.6	9.6 ± 0.56
3	[K34R]-GLP-1(7-37)-OH	**−11**	mono	0.148 ± 0.078	*b*	*b*	
4	[K34R]-GLP-1(7-37)-OH	−γGlu- indomethacin	mono	0.068 ± 0.037	58.6 and N/A[c]	15.2 and N/A[c]	
5	[K34R]-GLP-1(7-37)-OH	−O2Oc-indomethacin	mono	0.221 ± 0.109			
6	[K34R]-GLP-1(7-37)-OH	−K(**11**)-γGlu-indomethacin	dual	0.547 ± 0.211	N/A[c]	N/A[c]	21.6 ± 0.11
7	[K34R]-GLP-1(7-37)-OH	−O2Oc-K(**11**)-γGlu-indomethacin	dual	0.522 ± 0.265			
8	[K34R]-GLP-1(7-37)-OH	**−15**	mono	0.118 ± 0.081	32.1	11.6	

[a]Human GLP-1 receptor EC_{50} ± SEM were derived from three independent experiments carried out in triplicate (n = 3). Oligomeric states of **2**, liraglutide, **4**, **6**, and **8** were determined by SEC using a linear calibration curve. Supramolecular hydrodynamic radii (r_H) of liraglutide and **6** were determined by DLS and reported as mean ± SEM of the quadratic fits derived from cumulant analysis, n = 5. [b]In the SEC study, **3** was substituted for **8** (Supporting Information, Figure 13) due to an acute lack of peptide. [c]self-assembly size exceeded detection limits.

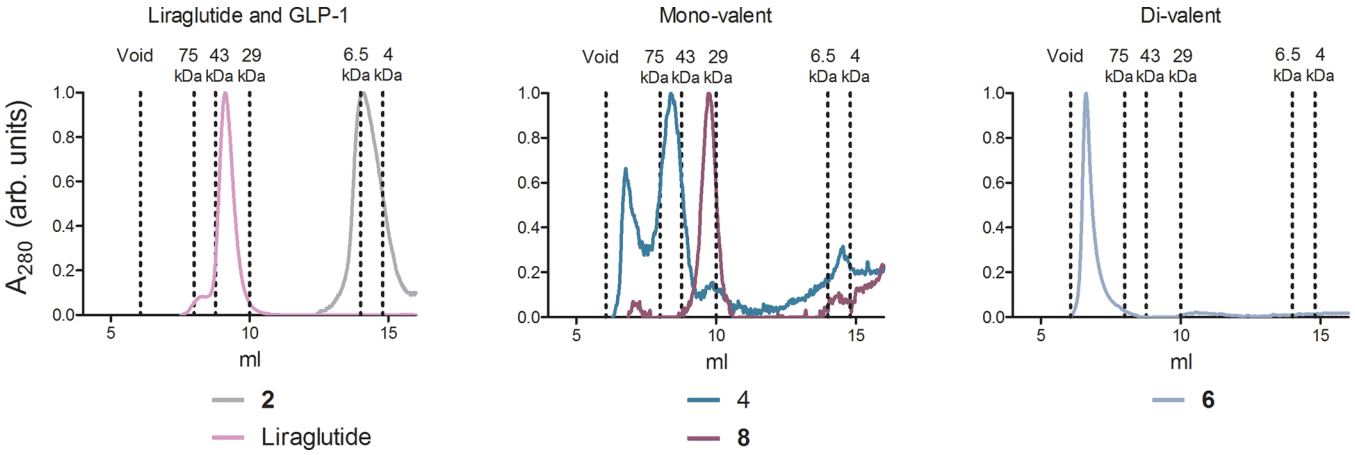

Figure 1. Size exclusion chromatograms of GLP-1 analogues (100 μL, 1 mg/mL) divided into three separate chromatograms; the controls, **2**, and liraglutide are displayed to the left, monovalent GLP-1 analogues at the center, and divalent **6** to the right. Compound **8** was used as an analogue of **3**. The *x*-axis marks the retention volume, while the *y*-axis marks the eluate absorption at 280 nm normalized for clarity. Retention volume and apparent size of molecular markers are depicted by dotted lines.

changed the GLP-1 receptor potency. All analogues were found to be full GLP-1 agonists with subnanomolar functional activities (Table 1 and Supporting Information, Figure 15). In general, the monovalent analogues (**3**−**5**, and **8**) demonstrated activity toward the GLP-1 receptor in the low nanomolar area, showing only slight reductions in potencies as a consequence of conjugation. Meanwhile, the divalent GLP-1 analogues (**6** and **7**) demonstrated a more profound reduction in GLP-1 activity compared to native GLP-1 (**1**) and their backbone peptide (**2**).

Biophysical Characterization. *Size Exclusion Chromatography.* The self-assembly of peptides to form noncovalent oligomers can affect absorption rates as well as circulatory half-lives. It is thus important to study whether the introduction of a small molecule on the peptide affects GLP-1 self-assembly. Hence, the divalent GLP-1 analogue **6** and two monovalent GLP-1 analogues containing a diflunisal- or indomethacin-like moiety, respectively, were submitted to SEC and compared to their backbone peptide (**2**) and liraglutide (Figure 1 and Table 1).

Peptide **2** was found to elute as a single, broad peak with a retention volume of 14.1 mL, which corresponded to an apparent molecular weight of 5 kDa (m = 1.5). This indicated that in solution the liraglutide backbone peptide, **2**, existed as a mix of monomers and dimers. Liraglutide was found with a V_R of 9.1 mL, corresponding to a supramolecule with an apparent molecular weight of 43 kDa and an oligomeric state of 11.6. Liraglutide has previously been shown to form a heptamer at pH 8 and in the presence of 100 mM NaCl.[29]

Like liraglutide, both monovalent- and divalent GLP-1 analogues exhibited self-assembly, albeit to different degrees. Monovalent diflunisal-containing GLP-1 analogue **8** (Supporting Information, Figure 13), substituting for analogue **3** due to an acute lack of compound, eluted as a single peak with a V_R of 9.8 mL, which translated to an apparent molecular weight of 32 kDa (m = 8.8). Meanwhile, the indomethacin-containing monovalent peptide **4** eluted in a polydisperse fashion with two main peaks, of which the largest was at a V_R of 8.4 mL, corresponding to an apparent molecular weight of 59 kDa (m = 15.2). The second largest peak was at V_R of 6.8 mL, corresponding to a supramolecular size far beyond the upper limit of the standard curve. The divalent GLP-1 analogue **6** eluted with a V_R of 6.6 mL, also exceeding the limits of the column.

Aside from the described main peaks, the monovalent peptides **8** and, to a higher degree, **4**, also have less well-defined

DOI: 10.1021/acs.jmedchem.7b00787
J. Med. Chem. 2017, 60, 7434−7446

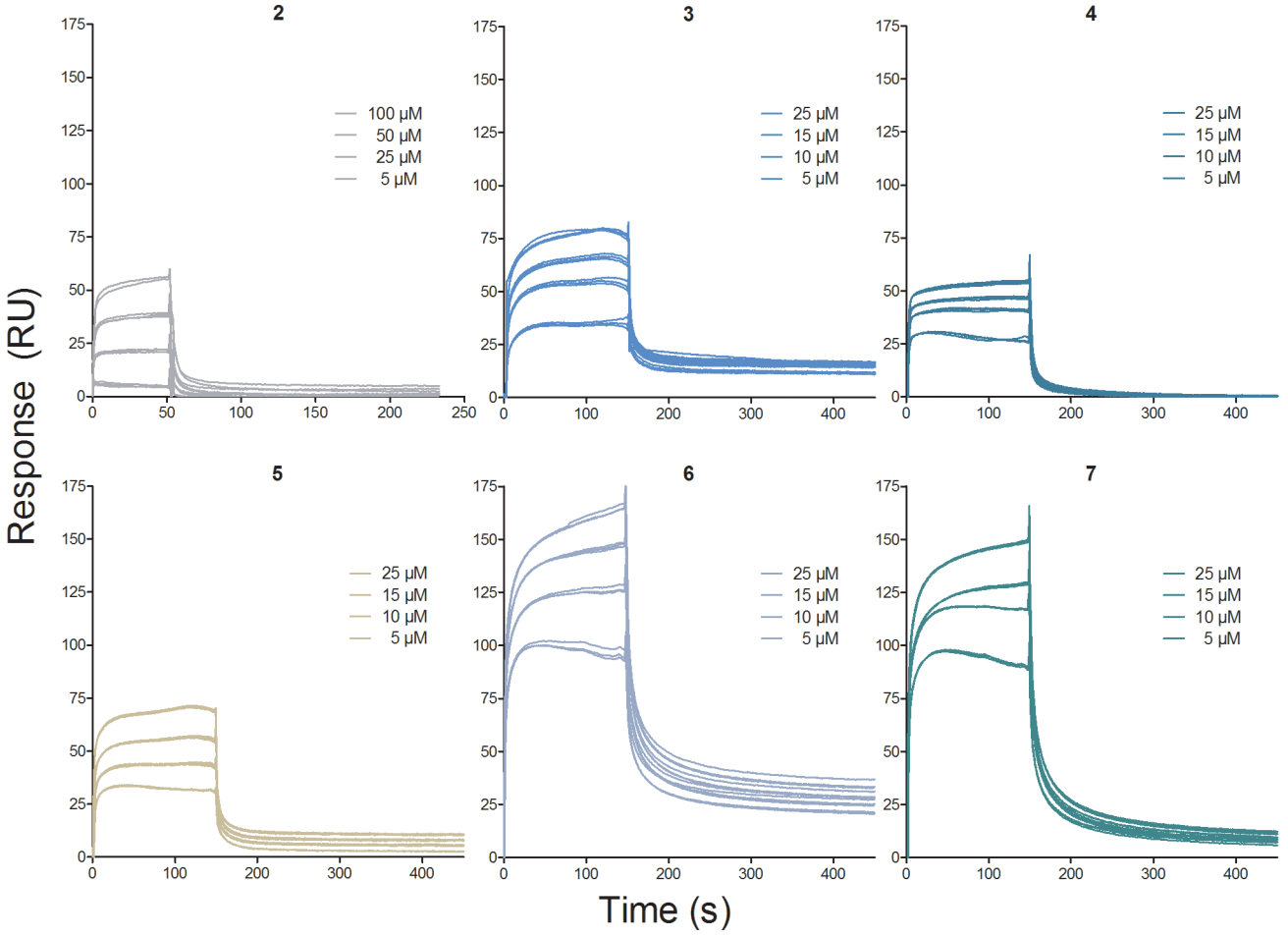

Figure 2. HSA interactions with GLP-1 analogues **2**–**7**. Sensorgrams were obtained from triple injections of peptides **3**–**7** (5–25 μM) and double/triple injections of **2** (1–100 μM) over a surface of 3555 RU immobilized HSA. Double referencing was used in all experiments.

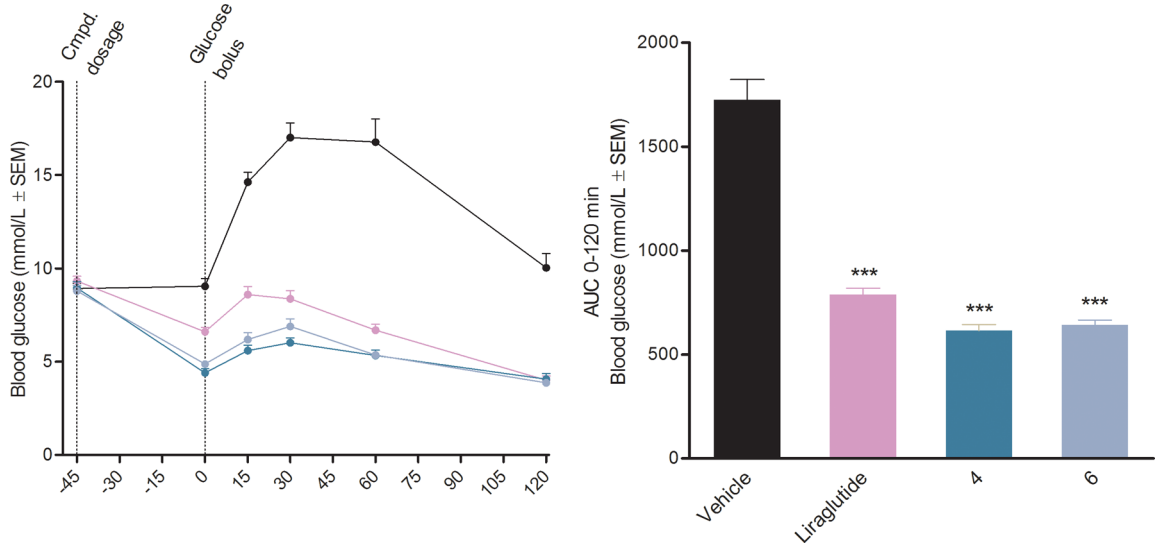

Figure 3. Oral glucose tolerance test on lean mice administered sc with vehicle, liraglutide, **4**, or **6**. Each group (n = 7) was dosed at t = −45 min (5 mL/kg, 10 nmol/mL). (left) Blood glucose in mmol/L ± SEM. (right) Area under the curve for the OGTT from 0 to 120 min. Asterisks represents P values below 0.001 derived from a one-way ANOVA analysis with Bonferroni's posthoc test.

eluent peaks, especially at 14–16 mL (apparent molecular weights 2.2–5.3 kDa, m = 0.6–1.5). This indicates that the monovalent peptides assembled in several states of more or less organized structures. Contrary to this, the lone peak derived from the divalent peptide **6** points to the formation of a single, well-ordered structure.

Dynamic Light Scattering. Divalent GLP-1 analogue **6** supramolecular self-assembly exceeded the limits of the SEC

DOI: 10.1021/acs.jmedchem.7b00787
J. Med. Chem. 2017, 60, 7434–7446

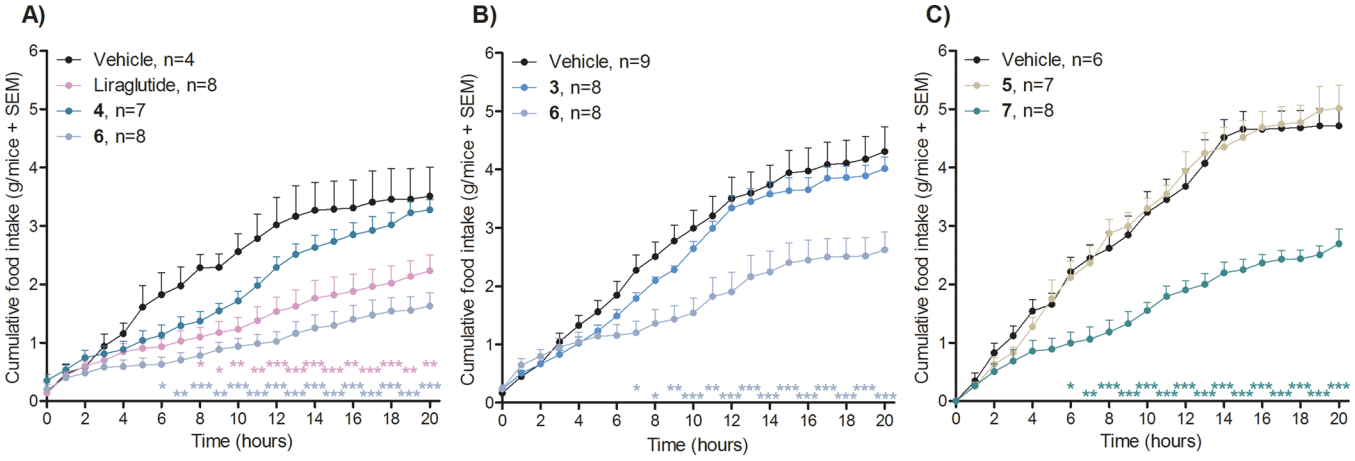

Figure 4. Cumulated food intake of mice (g/mouse) administered sc with vehicle or a GLP-1 analogue (5 mL/kg, 10 nmol/mL). (A–C) Three separate experiments. Two-way ANOVA with Bonferroni's posthoc test was used to compare food intake of treatment groups against the vehicle group. The asterisks *, **, and *** represents *P* values below or equal to 0.05, 0.01, and 0.001, respectively.

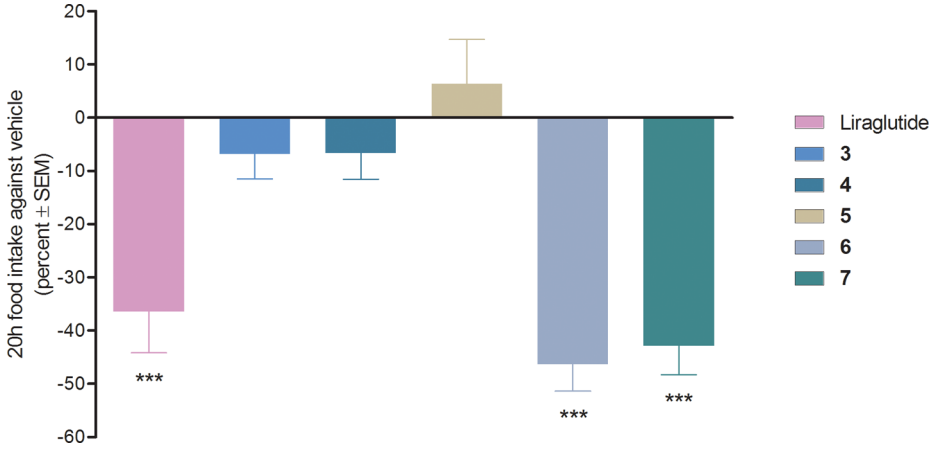

Figure 5. Twenty hours of cumulated food intake of mice (g/mouse ± SEM) administered sc with vehicle or a GLP-1 analogue (5 mL/kg, 10 nmol/mL). A one-way ANOVA analysis with Bonferroni's posthoc test was used to compare treatment groups to the vehicle animals. The asterisks represent *P* values below or equal to 0.001.

experiments. Thus, its hydrodynamic radius (r_H) was instead determined by dynamic light scattering (DLS). As a control, liraglutide r_H was investigated as well. As in the SEC experiment, DLS data analysis indicated monodisperse self-assembly of both liraglutide and **6** in solution (data not shown). The quadratic fit of second-order cumulant analysis were used to determine r_H. Supramolecular r_H of liraglutide and **6** was 9.6 ± 0.56 and 21.6 ± 0.11 nm, respectively, with narrow size distributions, as indicated by their low polydispersity indexes of 0.24 ± 0.01 and 0.19 ± 0.01. Thus, in PBS buffer, pH 7.4, at 1 mg/mL, the divalent GLP-1 analogue **6** self-assembled into an oligomer of far greater size than the liraglutide supramolecule.

Surface Plasmon Resonance (SPR). Immobilized HSA interacting with GLP-1 analogues **2**–**7**, in solution, were investigated using Biacore (Figure 2). A qualitative inspection of data revealed a remarkably high dissociation rate of the liraglutide peptide backbone, **2**, from HSA, indicating a weak, nonspecific binding. Compared to **2**, peptides **3** and **4** gave rise to higher concentration dependent responses and somewhat protracted dissociation rates (following an initial steep decline). Hence, the monovalent GLP-1 analogues appear to have increased albumin affinity compared to their backbone peptide. The divalent GLP-1 analogue **6** exhibited a further increase in concentration dependent responses and dissociation rate protraction. Hence, Biacore indicated that the divalent GLP-1 analogue **6** had a higher albumin affinity than its monovalent equivalents **3** and **4**. Meanwhile, comparing data from GLP-1 analogues with/without O2Oc revealed that, in this case, the spacer did not have beneficial effects on albumin affinity.

To determine equilibrium constants from Biacore data, interactions generally must follow a classic 1:1 binding pattern. However, the observed interactions between GLP-1 analogues **3**–**7** and HSA follow more complicated binding patterns of both (i) a nonspecific binding responsible for the initial, steep decline of the dissociation curve, and (ii) a slow dissociation symptomatic for high-affinity interactions. Such complicated interaction kinetics makes determination of kinetic constants unreliable.[30] Thus, kinetic constants and modeled best fits are not included.

Acute Effects in Vivo. *Oral Glucose Tolerance Test (OGTT).* An OGTT was performed to examine effects of the GLP-1 analogues on glucose homeostasis (Figure 3). The OGTT comprised four groups of mice treated with either a mono- or divalent GLP-1 analogue (peptide **4** or **6**), vehicle, or liraglutide (5 mL/kg, 10 nmol/mL). Mice were sc dosed 45 min prior to the administration of a glucose bolus. As compared

DOI: 10.1021/acs.jmedchem.7b00787
J. Med. Chem. 2017, 60, 7434–7446

to the glucose baseline of vehicle controls, the blood glucose (BG) levels in mice treated with either of the GLP-1 analogues were significantly reduced at time 0 ($P < 0.05$ for vehicle vs liraglutide, and $P < 0.001$ for vehicle vs peptides **4** and **6**). Furthermore, the positive control liraglutide significantly blunted OGTT-evoked BG increases compared to the vehicle (AUC 0−120 min; liraglutide 788 ± 84 mmol/L, vehicle 1725 ± 257 mmol/L, $P < 0.001$). The same applied to GLP-1 analogues **4** and **6**, which reduced BG excursion levels to the same level as liraglutide (AUC 0−120 min: for **4**, 614 ± 80 mmol/L; for **6**, 642 ± 66 mmol/L; $P < 0.001$ vs vehicle).

Food Intake. Food intake of lean mice was monitored over 20 h to examine the appetite-regulating effects of the GLP-1 analogues. The first food intake study comprised four groups of mice treated with either a mono- or divalent GLP-1 analogue (**4** or **6**), vehicle, or liraglutide (5 mL/kg, 10 nmol/mL) (Figure 4A). Compared to vehicle-dosed animals, mice treated with the positive control liraglutide consumed significantly less food over the course of 20 h (liraglutide 2.23 ± 0.27 g/20 h ($n = 8$), vehicle 3.51 ± 0.49 g/20 h ($n = 4$), $P < 0.001$). The effects of liraglutide on food intake was evident 4−5 h after administration and lasted throughout the study. Treatment with mono- or divalent GLP-1 analogues **4** and **6** showed different effects on acute food intake. The monovalent **4** did not reduce food intake compared to vehicle controls, and while **4** tended to reduce food intake in the first half of the study, the effect wore off in the second half. In contrast, the divalent GLP-1 analogue **6** promoted a significant reduction in food intake throughout the study (**6**: 1.62 ± 0.23 g/20 h ($n = 8$), $P < 0.001$ vs vehicle) with similar temporal pharmacodynamics as for liraglutide.

To compare the effects of GLP-1 analogues **3**−**7**, two additional food intake studies were performed (Figure 4B,C). None of the monovalent GLP-1 analogues, **3**−**5**, had a significant effect on the cumulated food intake during the 20 h study period (Figure 5). In contrast, both divalent GLP-1 analogues (**6** and **7**) lead to significant reductions in cumulated food intake.

Pharmacokinetics in Lean Mice. The PK profiles of one mono- and one divalent GLP-1 analogue (**4** and **6**) were investigated. Lean mice were administered sc (5 mL/kg, 10 nmol/mL) and blood sampled at eight time-points within 24 h. Plasma concentrations of GLP-1 analogues **4** and **6** were determined by LOCI-technology and are shown on Figure 6.

The PK analysis revealed a significant enhancement of in vivo half-life for the divalent GLP-1 analogue **6** compared to its monovalent equivalent **4**. The monovalent GLP-1 analogue **4** had a circulatory half-life of 55 min, while the divalent GLP-1 analogue **6** exhibited a circulatory half-life of 299 m.

Besides the prolonged half-life, the absorption of the divalent GLP-1 analogue **6** was significantly protracted compared to the monovalent GLP-1 analogue **4**. While blood concentrations of **4** had peaked 0.5 h after administration, the blood concentrations of **6** peaked around 4 h after administration. In summary, the attachment of a second small-molecule HSA ligand to a GLP-1 analogue dramatically increased half-life and protracted absorption rates in vivo.

DISCUSSION

Peptides are subject to extensive enzymatic degradation and rapid renal clearance. Consequently, half-life extension is a prerequisite for the development of many peptide pharmaceuticals. In this study, a novel method for peptide half-life extension using multivalent small-molecule albumin binders was explored and demonstrated for GLP-1 analogues.

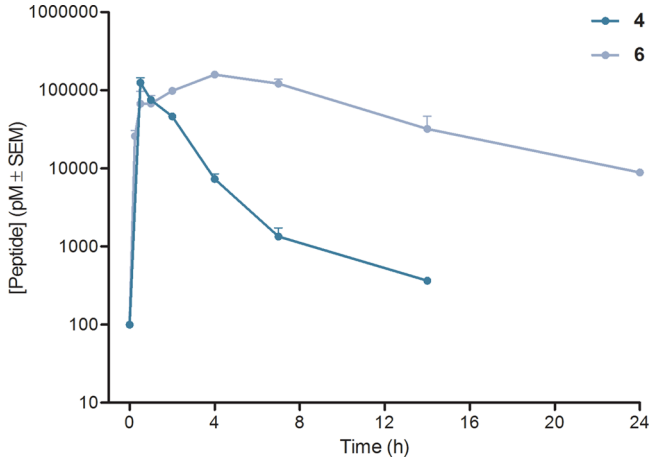

Figure 6. Pharmacokinetic profiles of **4** and **6** administered sc in C57bl/6 mice (5 mL/kg, 10 nmol/mL). Each time point equals three mice, and peptide concentrations were measured in triplicate. Error bars are shown when larger than the symbols representing data.

Five novel GLP-1 analogues with albumin binding motives were successfully synthesized. The ability of the selected small-molecule albumin ligands to confer HSA affinity to GLP-1 were studied by Biacore. Qualitative inspection of the data indicated that the small-molecule binders did indeed confer albumin affinity to GLP-1. Specifically, dissociation from albumin was protracted for the monovalent GLP-1 analogues compared to their backbone peptide, **2**. Rewardingly, the dissociation rates were further decreased for the divalent GLP-1 analogues, indicating higher albumin binding affinities compared to the monovalent GLP-1 analogues.

Peptide self-assembly can dramatically alter subcutaneous absorption rates. As a consequence, self-assembly often affects pharmacokinetic profiles of peptide pharmaceuticals.[29,31,32] For example, multimerization of liraglutide plays a role in its protracted absorption, which is important for its prolonged efficacy.[29] Here we observed how conjugation of either a diflunisal- or an indomethacin moiety to GLP-1 promoted self-assembly. The effect was further emphasized by the simultaneous introduction of both HSA ligands, i.e., SEC experiments indicated that divalent analogue **6** exhibited larger supramolecular structures than its monovalent equivalents. DLS experiments supported that **6** indeed self-assembled into large structures and that its supramolecular size far exceeded that of liraglutide. Whether this is a general characteristic of the divalent ligand or due to this particular combination of peptide sequence and small molecules remains to be studied.

To further quantify the properties of our small-molecule functionalized GLP-1 analogues, their receptor potencies were evaluated. Functional screening showed that the attachment of single HSA ligands slightly decreased GLP-1 receptor potency and that the divalent albumin ligands decreased GLP-1 receptor potency further. This correlation between modification size and potency decrease could be the result of increased steric hindrance. A similar pattern has been observed for the acylation of native GLP-1 with single-chain fatty acids versus bulky fatty acids.[33] However, this standard assay contained 0.1% BSA and the observed differences in GLP-1 receptor potency could also originate from variations in albumin affinities. Similar albumin concentrations are known to greatly impact GLP-1 receptor

DOI: 10.1021/acs.jmedchem.7b00787
J. Med. Chem. 2017, 60, 7434−7446

binding of liraglutide and other lipidated GLP-1 analogues.[34] The introduction of a spacer between the peptide and a bulky half-life extender has been used to circumvent potency-lowering effects of the bulky molecule.[33] Interestingly, introduction of an O2Oc spacer between GLP-1 and the albumin ligands had no effect on potency for our compounds. This could indicate that the observed decreases in GLP-1 receptor potencies were primarily caused by albumin interactions.

Selected GLP-1 analogues were further evaluated in an OGTT, which demonstrated their blood glucose lowering efficacies and supported the in vitro results regarding subnanomolar functionality. The OGTT data showed that both monovalent analogue **4** and divalent analogue **6** decreased blood glucose levels with similar efficacy as compared to liraglutide. Accordingly, the slightly lower potencies observed for GLP-1 analogues with divalent ligands compared to monovalent ligands did not negatively impact efficacy at pharmacological doses in mice.

The small-molecule functionalized GLP-1 analogues were also investigated for inhibitory effects on food intake, and here, a superior efficacy of the divalent GLP-1 analogues was evident. Monovalent GLP-1 analogues had minimal effects on feeding over the course of 20 h. In contrast, the divalent GLP-1 analogues significantly reduced food intake. This difference in efficacy between the mono- and divalent peptides was presumably related to different pharmacokinetics, as the OGTT revealed how both mono- and divalent peptides were fully active in vivo. Hence, the lack of robust anorectic effects of monovalent GLP-1 analogues were probably due to relatively short circulatory half-lives, as compared to the divalent GLP-1 analogues. This hypothesis was supported by a subsequent study investigating the PK properties of **4** and **6**.

In C57Bl/6 mice, we found the circulatory half-life of the monovalent GLP-1 analogue **4** to be 55 min. A 55 min half-life is longer than would be expected for native GLP-1 because mice do not have subcutaneous fat to protract absorption and GLP-1 is metabolized almost instantaneously in plasma by DPP-IV (native GLP-1 $t_{1/2}$ < 2 min, human iv). Hence, this study confirms findings in the literature[10−14] that monovalent small-molecule HSA ligands can be utilized for peptide half-life extension. Importantly, we found the half-life of the divalent GLP-1 analogue **6** to be more than five times longer than that of the corresponding monovalent analogue **4**. Peptide **6** had a half-life of 299 min, demonstrating that divalent small-molecule albumin binders can significantly prolong peptide half-life, as compared to their monovalent counterparts.

The observed PK properties of **6** could be explained by a dual mode-of-action comprising initial local drug deposition followed by albumin binding. It may be speculated that self-assembly or aggregation of **6** could lead to the formation of relatively stable depots at the subcutaneous injection site, from which the peptide would be slowly released to circulation. Once in circulation, **6** could bind albumin with high avidity, which would protect the peptide against degradation and renal clearance. Similar dual mode-of-actions are known for a number of other peptide pharmaceuticals, including liraglutide.[35] For liraglutide, this combination of absorption protraction and half-life extension leads to its continuous efficacy at once-daily sc administration in humans (t_{max} 9−13 h, $t_{1/2}$ 13 h).[35] As liraglutide and the divalent GLP-1 analogue **6** have similar PK properties in mice (sc: t_{max} 6 h and $t_{1/2}$ 4.4 h[36] vs t_{max} 4 h and $t_{1/2}$ 5 h), it is feasible that peptide **6** is suitable for once-daily treatments.

CONCLUSION

Novel GLP-1 analogues with covalently attached mono- and divalent small-molecule albumin binders were synthesized. In vitro characterization studies supported the ability of monovalent small-molecule albumin binders to confer HSA affinity. The unprecedented divalent small-molecule albumin binders had a significantly increased affinity for albumin, which confirmed our original design. As a consequence of enhanced PK properties, divalent GLP-1 analogues exhibited superior in vivo efficacy compared to their monovalent analogues. In solution, the small-molecule binders directed self-assembly of the GLP-1 analogues, which may be important for eventual sc absorption rates. This study demonstrates a novel method for in vivo half-life extension of peptide pharmaceuticals, specifically, how divalent small-molecule albumin binders can promote longer-lasting in vivo efficacy of GLP-1 analogues. Further customization of the divalent albumin binder in applications for specific peptides and proteins can be envisioned. This could include changing the linker, adding additional HSA ligands, replacing functional groups of the ligands, replacing the ligand moieties themselves, and so forth. We find that divalent small-molecule albumin binders have a significant potential as alternatives to PEGylation and lipidation.

EXPERIMENTAL SECTION

Materials. Synthesis and purification: *N*,*N*′-dicyclohexylcarbodiimide (DCC), dichloromethane (DCM), 4-(dimethylamino)pyridine (DMAP), *tert*-butanol (*t*BuOH), heptane, indomethacin crystalline, 4-hydroxy-[1,1′-biphenyl]-3-carboxylic acid (diflunisal-desfluoro), ethyl acetate (EtOAc), potassium carbonate (K_2CO_3), *N*,*N*-dimethylformamide (DMF), benzyl bromoacetate, magnesium sulfate ($MgSO_4$), palladium hydroxide on carbon ($Pd(OH)_2/C$), Celite, borane dimethylamine complex, tetrakis(triphenylphosphine)palladium(0), triethylsilane (TES), diethyl ether (Et_2O), acetonitrile (MeCN), sodium carbonate (Na_2CO_3), diflunisal, formic acid, and molecular sieves were purchased from Sigma-Aldrich (Brøndby, Denmark). *N*-[(1*H*-Azabenzotriazol-1-yl)(dimethylamino)methylene]-*N*-methylmethanaminium hexafluorophosphate *N*-oxide (HATU), *N*-[(1*H*-benzotriazol-1-yl)(dimethylamino)methylene]-*N*-methylmethanaminium hexafluorophosphate *N*-oxide (HBTU), and 1-hydroxy-7-azabenzotriazol (HOAt) were purchased from GL Biochem Ltd. (Shanghai, China). *N*,*N*′-Diisopropylcarbodiimide (DIC), 1-methylimidazole (MeIm), *N*-methyl-2-pyrrolidone (NMP), *N*,*N*-diisopropylethylamine (DIPEA), piperidine, trifluoroacetic acid (TFA), Fmoc-8-amino-3,6-dioxaoctanoic acid (Fmoc-O2Oc-OH), and all Fmoc- or Boc-protected amino acids were purchased from Iris Biotech GmbH (Marktredwitz, Germany). Sodium acetate (NaOAc) was acquired from Merck Millipore (Darmstadt, Germany), while Wang functionalized TentaGel S PHB resin (0.27 mmol/g) and Rink functionalized TentaGel S RAM (0.22 mmol/g) was purchased from Rapp Polymere GmbH (Tübingen, Germany).

Human GLP-1 receptor activation assay: Growth medium (DMEM with glutaMAX-I and 4.5 g/L D-glucose), fetal bovine serum, penicillin and streptomycin, Geneticin (G418), Hank's Balanced Salt Solution (HBSS), and PBS without calcium chloride ($CaCl_2$) and magnesium chloride ($MgCl_2$) were all purchased from Gibco (Thermo Fisher Scientific, Hvidovre, Denmark). Zeocin was purchased from Invitrogen (Thermo Fisher Scientific, Hvidovre, Denmark). HEPES, $MgCl_2$, $CaCl_2$, bovine serum albumin, and cell dissociation solution (non-enzymatic) were purchased from Sigma-Aldrich (Brøndby, Denmark). The 384-well format black sterile microplates were purchased from BD Falcon (USA). Excitation filter CFP 430/24 (X430), emission filters FITC 535/25 (M535), and CFP 470/24 (M470) as well as a CFP/YFP D450_515 single mirror were purchased and placed in an Envision 2104 multilabel reader (PerkinElmer, Skovlunde, Denmark).

DOI: 10.1021/acs.jmedchem.7b00787
J. Med. Chem. 2017, 60, 7434−7446

Size exclusion chromatography, dynamic light scattering, and surface plasmon resonance biosensing: Molecular weight standards aprotinin, ribonuclease, carbonic anhydrase, and ovalbumin were purchased from GE Healthcare (Denmark) and vitamin B12 from Sigma-Aldrich (Brøndby, Denmark), while peptide YY_{3-36} was produced in-house. Gibco PBS buffer, pH 7.4, was purchased from Life Technologies (The Netherlands). *N*-Hydroxysuccinimide (NHS), ethanolamine, sodium hydroxide (NaOH), dimethyl sulfoxide (DMSO), and 1-ethyl-3-(3-(dimethylamino)propyl)carbodiimide (EDC), as well as HSA essentially fatty acid free, were purchased from Sigma-Aldrich (Brøndby, Denmark).

Diflunisal-Linker Synthesis. *General.* ^{1}H, ^{13}C, and HMQC NMR spectra were recorded using a Bruker Avance 300 spectrometer with a BBO probe. The chemical shifts were referenced to the residual solvent signal. Column chromatography on silica gel was performed on a Biotage Isolera Spektra One instrument using SNAP HP-SIL columns. Mass determination (high-resolution MS, HRMS) was performed on a Bruker SolariX XR instrument (Bruker, Bremen, Germany) with ESI and MALDI probes.

*tert-Butyl 2′,4′-Difluoro-4-hydroxy-[1,1′-biphenyl]-3-carboxylate (**9**).* A solution of DCC (1.073 g, 5.200 mmol) in DCM (10 mL) was added to a mixture of diflunisal (1.000 g, 3.997 mmol) and DMAP (0.488 g, 3.994 mmol) in toluene/DCM/*t*BuOH 1:4:4 (45 mL). The resulting suspension was stirred at room temperature for 2.5 days. After that, it was filtered and the solvent was evaporated under reduced pressure. The crude was purified by column chromatography on silica gel using a Biotage Isolera Spektra One (SNAP HP-SIL 50 g, heptane/EtOAc 0% to 0% 3CV, 0% to 15% 22 CV) to obtain **9** (0.857 g, 70%) as a white solid. ^{1}H NMR (300 MHz, $CDCl_3$) δ 11.14 (s, 1H, OH), 7.90 (dd, $^{4}J_{2,6}$ = 2.2, $^{5}J_{H-F}$ = 1.3 Hz, 1H, H_{ar}-2), 7.61−7.52 (m, 1H, H_{ar}-6), 7.38 (ddd, $^{3}J_{5'-6'}$ = 8.8, $^{4}J_{H-F}$ = 6.6, 1H, H_{ar}-6′), 7.04 (d, $^{3}J_{5,6}$ = 8.6 Hz, 1H, H_{ar}-5), 7.01−6.86 (m, 2H, H_{ar}-3′+5′), 1.64 (s, 9H, CH_3). ^{13}C NMR (75 MHz, $CDCl_3$) δ 169.8 (s, CO), 162.7 (dd, $^{1}J_{C-F}$ = 181.7, $^{3}J_{C-F}$ = 11.6 Hz, C_{ar}-F), 161.6 (s, C_{ar}-4), 159.4 (dd, $^{1}J_{C-F}$ = 182.5, $^{3}J_{C-F}$ = 11.8 Hz, C_{ar}-F), 135.8 (d, $^{4}J_{C-F}$ = 2.9 Hz, C_{ar}- 6), 131.2 (dd, $^{3}J_{C-F}$ = 9.4, 4.8 Hz, C_{ar}-6′), 130.5 (d, $^{4}J_{C-F}$ = 2.8 Hz, C_{ar}-2), 125.9 (d, $^{3}J_{C-F}$ = 0.9 Hz, C_{ar}-1), 124.6 (dd, $^{2}J_{C-F}$ = 13.8, $^{4}J_{C-F}$ = 3.8 Hz, C_{ar}-1′), 117.9 (s, C_{ar}-5), 114.1 (s, C_{ar}-3), 111.7 (dd, $^{2}J_{C-F}$ = 21.1, $^{4}J_{C-F}$ = 3.9 Hz, C_{ar}-5′), 104.5 (dd, $^{2}J_{C-F}$ = 26.6, 25.3 Hz, C_{ar}-3′), 83.4 (s, $C(CH_3)_3$), 28.3 (s, CH_3). HRMS (ESI): calcd for $C_{17}H_{17}F_2O_3$ $[M + H]^+$ 307.1146, $C_{17}H_{16}F_2O_3Na$ $[M + Na]^+$ 329.0965; found 307.1140, 329.0960.

*tert-Butyl 4-(2-(benzyloxy)-2-oxoethoxy)-2′,4′-difluoro-[1,1′-biphenyl]-3-carboxylate (**10**).* K_2CO_3 (632 mg, 4.573 mmol) was added to a solution of **9** (700 mg, 2.285 mmol) in DMF (8 mL), and the resulting mixture was stirred at room temperature for 5 min. After that, benzyl bromoacetate (542 μL, 3.431 mmol) was added, the temperature was raised to 45 °C, and the reaction was stirred for 2 h. Afterward, the reaction was diluted with 50 mL of EtOAc and washed with brine (3 × 50 mL). The organic phase was dried over $MgSO_4$, filtered, and the solvent removed under reduced pressure. The crude was purified by column chromatography on silica gel using Biotage Isolera Spektra One (SNAP HP-SIL 50 g, heptane/EtOAc 0% to 0% 3CV, 0% to 10% 25 CV) to obtain **10** (1.031 g, 99%) as a colorless viscous oil. ^{1}H NMR (300 MHz, $CDCl_3$) δ 7.86 (dd, $^{4}J_{2,6}$ = 2.3, $^{5}J_{H-F}$ = 1.2 Hz, 1H, H_{ar}-2), 7.51 (ddd, $^{3}J_{5,6}$ = 8.6, $^{4}J_{2,6}$ = 2.3, $^{5}J_{H-F}$ = 1.8 Hz, 1H, H_{ar}-6), 7.43−7.31 (m, 6H, H_{ar}-6′+Bn), 7.01−6.85 (m, 3H, H_{ar}-3′+5′+5), 5.26 (s, 2H, PhCH_2), 4.78 (s, 2H, COCH_2O), 1.60 (s, 9H, CH_3). ^{13}C NMR (75 MHz, $CDCl_3$) δ 168.5 (s, CO), 165.2 (s, CO), 162.8 (dd, $^{1}J_{C-F}$ = 194.1, $^{3}J_{C-F}$ = 11.7 Hz, C_{ar}-F), 159.5 (dd, $^{1}J_{C-F}$ = 195.3, $^{3}J_{C-F}$ = 11.8 Hz, C_{ar}-F), 156.8 (s, C_{ar}-4), 135.3 (s, C_{ar}-Bn_{ipso}), 133.1 (d, $^{4}J_{C-F}$ = 3.3 Hz, C_{ar}-6), 132.0 (d, $^{4}J_{C-F}$ = 2.4 Hz, C_{ar}-2), 131.3 (dd, $^{3}J_{C-F}$ = 9.5, 4.8 Hz, C_{ar}-6′), 128.8 (s, C_{ar}-Bn), 128.7 (s, C_{ar}-Bn), 128.6 (s, C_{ar}-Bn), 128.6 (d, $^{3}J_{C-F}$ = 0.7 Hz, C_{ar}-1), 124.1 (dd, $^{2}J_{C-F}$ = 13.6, $^{4}J_{C-F}$ = 3.9 Hz, C_{ar}-1′), 123.8 (s, C_{ar}-3), 114.5 (s, C_{ar}-5), 111.8 (dd, $^{2}J_{C-F}$ = 21.2, $^{4}J_{C-F}$ = 3.7 Hz, C_{ar}-5′), 104.6 (dd, $^{2}J_{C-F}$ = 26.4, 25.4 Hz, C_{ar}-3′), 81.8 (s, $C(CH_3)_3$), 67.2 (s, PhCH_2), 66.9 (s, COCH_2O), 28.4 (s, CH_3). HRMS (MALDI): calcd For $C_{26}H_{24}F_2O_5Na$ $[M + Na]^+$ 477.1489; found 477.1481.

*2-((3-(tert-Butoxycarbonyl)-2′,4′-difluoro-[1,1′-biphenyl]-4-yl)-oxy)acetic Acid (**11**).* **10** (490 mg, 1.078 mmol) was dissolved in EtOAc (6 mL) under H_2 flow. $Pd(OH)_2$/C (20 wt % loading, 60 mg, 0,085 mmol) was added and the resulting suspension stirred at room temperature for 1 h. Afterward, the suspension was filtered over Celite and the solvent removed under reduced pressure to obtain **11** (389 mg, 99%) as a white solid. ^{1}H NMR (300 MHz, $CDCl_3$) δ 7.95 (dd, $^{4}J_{2,6}$ = 2.2, $^{5}J_{H-F}$ = 1.2 Hz, 1H, H_{ar}-2), 7.71−7.61 (m, 1H, H_{ar}-6), 7.38 (ddd, $^{3}J_{5'-6'}$ = 8.7, $^{4}J_{H-F}$ = 6.4, 1H, H_{ar}-6′), 7.08 (d, $^{3}J_{5,6}$ = 8.6 Hz, 1H, H_{ar}-5), 7.02−6.88 (m, 2H, H_{ar}-3′+5′), 4.82 (s, 2H, CH_2), 1.63 (s, 9H, CH_3). ^{13}C NMR (75 MHz, $CDCl_3$) δ 169.7 (s, CO), 166.0 (s, CO), 162.9 (dd, $^{1}J_{C-F}$ = 213.3, $^{3}J_{C-F}$ = 11.9 Hz, C_{ar}-F), 159.6 (dd, $^{1}J_{C-F}$ = 213.9, $^{3}J_{C-F}$ = 11.9 Hz, C_{ar}-F), 157.8 (s, C_{ar}-4), 134.8 (d, $^{4}J_{C-F}$ = 2.9 Hz, C_{ar}-6), 132.4 (d, $^{4}J_{C-F}$ = 2.8 Hz, C_{ar}-2), 131.3 (dd, $^{3}J_{C-F}$ = 9.5, 4.7 Hz, C_{ar}-6′), 129.8 (d, $^{3}J_{C-F}$ = 0.9 Hz, C_{ar}-1), 123.7 (dd, $^{2}J_{C-F}$ = 13.7, $^{4}J_{C-F}$ = 4.0 Hz, C_{ar}-1′), 121.6 (s, C_{ar}-3), 116.4 (s, C_{ar}-5), 112.0 (dd, $^{2}J_{C-F}$ = 21.2, $^{4}J_{C-F}$ = 3.8 Hz, C_{ar}-5′), 104.7 (dd, $^{2}J_{C-F}$ = 26.3, 25.4 Hz, C_{ar}-3′), 83.6 (s, $C(CH_3)_3$), 68.5 (s, CH_2), 28.2 (s, CH_3). HRMS (ESI): calcd for $C_{19}H_{18}F_2O_5Na$ $[M + Na]^+$ 387.1020; found 387.1012.

Peptide Synthesis. *General.* Peptides were assembled using Fmoc-based SPPS and were purified by RP-HPLC on a Dionex Ultimate 3000 system (Thermo Scientific, Hvidovre, Denmark) with preparative C18 columns (300 Å, 5 μm, 21.5 mm × 250 mm; FeF Chemicals, Køge, Denmark). Solvent A consisted of milli-Q water and TFA (0.1%). Solvent B consisted of HPLC grade MeCN and TFA (0.1%). The gradient used for separation was a linear 5−70% B for 25 min.

Liraglutide was purchased as Victoza (6 mg/mL^{-1} formulation) and either used as such (for in vivo studies) or purified by preparative RP-HPLC prior to use (for functional screening and studies of physicochemical properties)

*Synthesis of GLP-1 Analogues **1** and **2**.* Peptide **1** and **2** were synthesized on 0.1 mmol and 2 × 0.5 mmol scale, respectively, using Fmoc-based SPPS. Peptide **1** was synthesized on a Rink-amide resin and **2** on a Wang functionalized resin. For peptide **2**, Fmoc-Gly-OH was anchored manually to a Wang functionalized resin by dissolving Fmoc-Gly-OH (10 equiv), DIC (5 equiv), and MeIm (5 equiv) per 1 equiv resin in 6 mL of DMF and 35 mL of DCM. The reaction was left on a plate shaker 12 h at room temperature, after which the resin was transferred to a fritted 20 mL syringe and washed with NMP (3×) and DCM (3×). This procedure was repeated, and the resin was dried 12 h in vacuo. The loading of the resin was 0.18 mmol/g.[37]

Peptide **1** and the remainder of **2** were synthesized using a fully automated Initiator+ Alstra automated microwave peptide synthesizer (Biotage, Sweden), where couplings were performed with Fmoc amino acids (5 equiv), HOAt (5 equiv), HBTU (4.75 equiv), and DIEA (9.75 equiv). Couplings 2−20 (C-to-N) were performed for 10 min at 75 °C. Fmoc-deprotection were carried out with piperidine/DMF (2:3) for 3 min and then piperidine/DMF (1:4) for 15 m. After each coupling and each Fmoc-deprotection, the resin was washed with NMP (3×), DCM (1×), and DMF (2×). The incorporation of amino acids 20−30 (C-to-N) were performed using double couplings under the same circumstances as well as an additional deprotection step with piperidine/DMF (1:4) for 15 min. Finally, the last amino acid of **2**, Boc-His(Trt)-OH, was attached by double couplings for 2 h at room temperature.

*Synthesis of GLP-1 Analogues **3**−**8**.* To synthesize GLP-1 analogues **3**−**8**, resin-bound Boc-[K34R]-GLP-1(7-37) was selectively elongated at the ε-amine of Lys26 using SPPS (Scheme 2). The Alloc group protecting the ε-amine of Lys26 was selectively removed using 1 equiv tetrakis(triphenylphosphine)palladium(0) and 1.5 equiv borane dimethylamine complex in DCM, which had been bubbled with argon gas. The resin was added to DCM (10 mL), and a flow of argon was applied to the mixture for 10 min before addition of the borane dimethylamine complex and an additional 10 min of argon flow. Subsequently, tetrakis(triphenylphosphine)palladium(0) was added and the reaction was left with argon bubbling for 2 h at room temperature. Afterward, the resin was washed sequentially with DCM (3×), NMP (3×), and DCM (3×). Adequate Alloc-removal was confirmed by a LCMS of a mini-cleavage (10 mg resin) made using 1

DOI: 10.1021/acs.jmedchem.7b00787
J. Med. Chem. 2017, 60, 7434−7446

mL of 95:2.5:2.5 TFA/TES/H_2O for 1 h at room temperature. The Alloc deprotected Boc-[K34R]-GLP-1(7-37) now contained a single free amine in the peptide.

The resin containing the Alloc deprotected Boc-[K34R]-GLP-1(7-37) was divided into portions of 0.1 mmol, on which the various steps for synthesis of peptides **3**−**8** were performed. Couplings were performed in DMF using HATU (5 equiv), DIEA (7.2 equiv), and amino acids/Fmoc-O2Oc-OH/indomethacin/**11** or **15** (4 equiv). Reactions were shaken for 8 h (150 rpm) at room temperature, after which they were washed with DMF (3×). The couplings were then repeated and left on the shaker O/N. Fmoc protected amines were deprotected using piperidine/DMF (2:5) for 3 min and piperidine/DMF (1:4) for 15 min, while Alloc groups were removed as described above. After coupling and deprotection steps, the resin was washed with NMP (3×), DCM (3×), and DMF (3×). The six GLP-1 analogues, **3**−**8**, were modified as follows. **3**: Coupling of **11**. **4**: Coupling of Fmoc-L-Glu-O*t*Bu, Fmoc-deprotection, and then the coupling of indomethacin. **5**: Coupling of Fmoc-O2Oc-OH, Fmoc-deprotection and then the coupling of **11**. **6**: Coupling of Fmoc-L-Lys(Alloc)-OH, Fmoc-deprotection, coupling of Fmoc-L-Glu-O*t*Bu, Fmoc-deprotection, and then the coupling of indomethacin. Afterward, the Alloc-group was removed and **11** coupled to N^{ε} of the lysine. **7**: Coupling of Fmoc-O2Oc-OH, Fmoc-deprotection, and then the same steps used to synthesize **6**. **8**: Coupling of **15**.

Peptide Purification. After synthesis, resins were washed with DMF (3×) and DCM (3×). Peptides **1**−**8** were then cleaved from the resin by treatment with TFA/TES/H_2O (95:2.5:2.5; 4 mL) for 15 min at room temperature, then another 4 mL for 2 h. Following cleavage, the TFA solutions were concentrated under nitrogen flow, and peptides were precipitated with Et_2O to yield a crude product. Finally, all peptides were purified by preparative RP-HPLC and analyzed by LCS as well as HRMS (except **1**, **2**, and liraglutide, which were not examined by HRMS).

Peptide Analysis. The peptides were analyzed on a Biotage Resolux 300 Å C18 column (5 μm, 150 mm × 4.6 mm) with a flow rate of 1.0 mL/min. Solvents consisted of A (milli-Q water and 0.1% formic acid) and B (LCMS grade MeCN and 0.1% formic acid). Peptides were eluted using a linear gradient of 5−70% of solvent B. LCMS revealed purities of ≥95% for all peptides, as determined by UV-absorption at 215 nm. Finally, ESI-MS-based identifications of peptides were confirmed by HRMS using a Bruker SolariX XR instrument (Bruker, Bremen, Germany) with ESI and MALDI probes. Results are shown in Supporting Information, Figures 1−12.

In Vitro Studies. *Human GLP-1 Receptor Activation Assay.* A stable HEK293 cell line expressing the Epac cAMP-sensor as well as the GLP-1 receptor was used for functional screening of the GLP-1 analogues. This cell line utilizes mCerulean and mCitrine attached to the Epac protein as fluorescence resonance energy transfer (FRET) pair and was previously described by Mathiesen and co-workers.[38] Cells were kept at 37 °C in DMEM growth medium supplemented with 10% heat-inactivated fetal bovine serum and 1% penicillin−streptomycin in a humidified 5% CO_2 incubator. Furthermore, 0.05 mg/mL zeocin and 0.5 mg/mL Geneticin was added to the growth medium to maintain selection pressure.

For the real-time cAMP signaling assays, cells were detached using nonenzymatic cell dissociation solution, spun down and resuspended in assay buffer (HBSS with 20 mM HEPES supplemented with 1 mM $CaCl_2$, 1 mM $MgCl_2$, and 0.1% albumin, pH 7.4) to a cell concentration of 10^5 cells per mL. Cells were then transferred to black 384-well microplates where ligands were added in the indicated concentrations. Immediately after, increases in cAMP levels were measured as increases in the mCerulean/mCitrine emission ratio using an Envision 2104 multilabel reader, with measurement starting from 1 min and continuing for 60 min after ligand addition. The energy donor mCerulean was excited using an optical filter CFP-430 (X430) and a CFP/YFP (D450_515) single mirror. Subsequently, emission from both the donor mCerulean and the acceptor mCitrine was measured using YFP-535 (M535) and CFP-470 (M470) filters. At the time point of maximum cAMP levels (30 min after addition of ligands), dose−response curves were generated and ligand EC_{50} values were calculated (Table 1 and Supporting Information, Figure 15).

Size Exclusion Chromatography. Samples (100 μL) were separated by size on a fast protein liquid chromatography instrument (ÄKTAPurifier100, GE Healthcare, Brøndby, Denmark) with a calibrated Superdex 75 10/300 column (Pharmacia, Uppsala, Sweden) at 10 °C using PBS pH 7.4 as running buffer and a flow rate of 0.45 mL min^{-1}. Column eluate was monitored at 280 nm using an UV detector. Apparent molecular weight was calculated from molecular weight standards using a linear calibration curve generated from a plot of retention volume versus log(MW) (Supporting Information, Figure 14). Peak heights were normalized to 1 for all compounds in a figure.

Dynamic Light Scattering. Samples (0.1 mg/mL in 0.1 mM PBS pH 7.4, 500 μL) of **6** or liraglutide were filtered into quartz cuvettes through 0.2 μm syringe filters (Whatman Anotop Plus, GE Healthcare, Brøndby, Denmark). Samples were analyzed at 25 °C using a DLS instrument consisting of a BI-200SM goniometer, a BI-APD Avalanche photodiode detector, a BI-9000AT digital autocorrelator, and a 632.8 nm HeNe laser with a power of 35 mW (Brookhaven Instruments Corp., New York, USA). Measurements were obtained as 5 acquisitions of 60 s. Data were analyzed using 9KDSLW software (Brookhaven Instruments Corp., New York, USA). A regularization algorithm (CONTIN) was applied initially to establish the presence of a monomodal size distribution, and second-order cumulant analysis was subsequently used to estimate the average hydrodynamic radius (r_H) of the particles via the Stokes−Einstein equation: $r_H = \frac{k_B T}{6\pi\eta D_\tau}$ where k_B is the Boltzmann constant, T is the absolute temperature, η is the viscosity of the solvent, and D_τ is the translational diffusion coefficient calculated from the intensity autocorrelation function.

Surface Plasmon Resonance Biosensing. Surface plasmon resonance analysis were performed at 25 °C using a setup described by Rich and co-workers[39] on a Biacore X100 with a CM5 sensor chip (GE Healthcare Biosciences AB, Uppsala, Sweden).

HSA was immobilized on the surface of the CM5 chip. The system was equilibrated with 10 mM PBS buffer, pH 7.4, at a flow rate of 10 μL/min, until a stable baseline was achieved. Flow cells 1 and 2 were activated for 7 min with a freshly prepared 1:1 mixture (v/v) of 1 M NHS and 1 M EDC. Subsequently, flow cell 1 was subjected to two injections of 30 μg/mL HSA in 10 mM NaOAc, pH 5.4, each lasting 7 min. Both flow cells were then capped by a 7 min injection of 1 M ethanolamine, pH 8.1. Finally, noncovalently bound HSA was removed with 3 × 12 s injections of 50 mM NaOH. The final amount immobilized corresponded to 3555 RU. The flow rate used for HSA attachment was 10 μL/min.

Interactions between the immobilized HSA and GLP-1 analogues **2**−**7** were studied at a flow rate of 30 μL/min using a running buffer of PBS buffer 10 mM with 3% DMSO, pH = 7.4. Peptides were dissolved in running buffer to prepare test samples, and concentrations were verified from UV absorption at 280 nm measured on a NanoDrop 2000 spectrophotometer (Thermo Fisher Scientific, Hvidovre, Denmark). All samples were measured in triplicate, and measurements were performed from low to high concentrations to minimize the risk of carryover between samples. Samples of GLP-1 analogues **3**−**7** were injected to the CM5 chip for 150 s, and the following dissociations were measured for 300 s. Peptide **2** was injected to the CM5 chip for 50 s, and dissociation was measured for 180 s. Between samples the surface was washed with 50 mM NaOH for 4 s and equilibrated with running buffer. It should be noted that each NaOH wash reduced the baseline by approximately 3 RU. Blanks were run every fifth sample.

In Vivo Studies. *Animals.* NMRI mice (25−30 g body weight (BW) (approximately 5 weeks old at the time of arrival) were obtained from Taconic (Lille Skensved, Denmark) and C57Bl/6 mice (20−25 g BW (6−8 weeks old) at the time of arrival) from Janvier Laboratories (Le Genest-Saint-Isle, France). Animals were group-housed (NMRI, 4 mice/cage; C57Bl/6, 5 mice/cage) in a light-, temperature-, and humidity-controlled room (12 h:12 h light:dark cycle, lights on/off at 02:00/14:00, 22 ± 1 °C; 50 ± 10% relative humidity). Animals had ad libitum access to regular chow diet (Altromin 1324, Brogaarden A/S, Denmark) and domestic quality tap water.

DOI: 10.1021/acs.jmedchem.7b00787
J. Med. Chem. 2017, 60, 7434−7446

All animal experiments were conducted in accordance with Gubra ApS bioethical guidelines, which were fully compliant to internationally accepted principles for the care and use of laboratory animals. The described experiments were covered by personal licenses for Jacob Jelsing (2013-15-2934-00784) issued by the Danish Committee for animal research.

Oral Glucose Tolerance Test. The acute effect of the peptides on glucose homeostasis were assessed by an oral glucose tolerance test. NMRI mice (n = 32), acclimatized for 5 days, were randomized into four groups (n = 8 per group) based on body weight prior to semifasting (day 0). Concomitant to randomization, cages were changed. Animals were fasted for 4 h, and at t = −30 min, mice were weighed and injected subcutaneously (sc, 5 mL/kg) with vehicle, peptide **2**, **4**, or **6** (10 nmol/mL). At t = 0, animals received an oral glucose load (200 mg glucose/mL (Fresenius Kabi, Uppsala, Sweden), dosing volume of 10 mL/kg) administered as a gavage via a gastrically placed tube connected to a syringe. Tail vein blood was sampled at −30, 0, 15, 30, 60, and 120 min in 10 μL heparinized glass capillary tubes and immediately suspended in 0.5 mL of buffer (glucose/lactate system solution, EKF-diagnostics, Barleben, Germany). Blood glucose was measured using a BIOSEN c-Line glucose meter (EKF-diagnostics) according to the manufacturer's instructions, and one-way ANOVA analysis with Bonferroni's posthoc tests were used to compare blood glucose levels between groups.

Food Intake. The acute effect of the peptides on the feeding behavior was assessed in three separate experiments with similar setup. NMRI mice were acclimatized for 5 days prior to dosing. The mice were group-housed (four mice/cage) in custom-made cages in which individual food intake can be measured (HM-2 system, MBRose, Faaborg, Denmark). Animal-allocated food intake was discriminated from spillage by defining a minimum bout size (>0.05 g) per entry.

Prior to study start, animals were randomized into four or three groups (n = 8−9) based on body weight. After randomization, mice were fasted from 8:00 to 14:00. Dosing was administrated sc (dose volume 5 mL/kg, 10 nmol/mL) in the lower back between 13:00 and 14:00 (just prior to lights off). After dosing, individual animal food intake was measured continuously for 20 h. One-way ANOVA analysis with Bonferroni's posthoc tests were performed to compare food intake between groups.

Pharmacokinetics. The 59 C57Bl/6 mice were acclimatized for 5 days and then randomized based on BW into four groups (untreated (n = 8), vehicle (n = 3), and two test groups treated with GLP-1 analogues **4** and **6** (n = 24)). GLP-1 analogues **4** and **6** were solubilized in 10 mM PBS with 0.1% BSA, pH 7.4, and animals were administrated sc (dose volume 5 mL/kg, 10 nmol/mL). Then 15 min post dosing, trunk blood was collected in separate Microvette 500 LH tubes (Sarstedt AG & Co, Nümbrecht, Germany) with 10 μL of 0.1 mM of the DPP-IV inhibitor linagliptin (Toronto Research Chemicals INC, Toronto, Canada) from three animals in the groups, which were treated with vehicle, peptide **4**, and **6**. Plasma was isolated by centrifugation, transferred to 0.5 mL Eppendorf Protein LoBind tubes (Eppendorf AG, Hamburg, Germany), and stored at −80 °C. For the treatment groups, this was repeated at seven set time-points over the course of 24 h. Blood from the untreated group was collected prior to dosing.

Peptide concentration was determined by a collaborator, Novo Nordisk A/S, using the luminescent oxygen channeling (LOCI) technology (Siemens Healthcare, Ballerup, Denmark). Plasma from the untreated groups were spiked with peptide **4** or **6** to create standard curves in the range of 200−300000 pM. Standard curves were made in duplicate. In vivo half-life was calculated using the exponential fitting "one-phase decay" in GraphPad Prism version 5.0 (San Diego, USA)

■ ASSOCIATED CONTENT

Supporting Information

The Supporting Information is available free of charge on the ACS Publications website at DOI: 10.1021/acs.jmedchem.7b00787.

LCMS chromatograms and HRMS of peptides, structure of compound **8**, SEC calibration data, in vivo activity curves from the functional screening experiments, and information regarding the synthesis of **15** (PDF)

■ AUTHOR INFORMATION

Corresponding Authors

*For K.J.J.: phone, +45 21516721); E-mail, kjj@chem.ku.dk.
*For S.L.P. phone, +45 31522650); E-mail: slp@gubra.dk.

ORCID

Mikkel B. Thygesen: 0000-0002-0158-2802
Knud J. Jensen: 0000-0003-3525-5452

Author Contributions

E.M.B., M.C.M., P.K.W., S.B.v.W., and M.B.T. performed the experiments. E.M.B., K.K.S., N.V., J.J., S.L.P., and K.J.J. discussed the data. E.M.B., S.L.P., and K.J.J. wrote the manuscript. All authors have given approval to the final version of the manuscript.

Notes

The authors declare the following competing financial interest(s): E.M.B., P.W.I., S.B.v.W., N.V., J.J., and S.L.P. are employees of Gubra ApS. J.J. and N.V. are major shareholders of Gubra ApS.

■ ACKNOWLEDGMENTS

The authors thank Dr. Christian Rosenquist, Dr. Suzi Høegh Madsen, and Susanne Halkier for analyzing blood samples used for PK analysis, Dr. Jesper Mosolff Mathiesen for providing the HEK293 cell line used for functional screening, and Dr. Søren Roi Midtgaard for aiding with SEC and DLS experiments. Mie Fabricius Wöldike and Prof. Hans Bräuner-Osborne are thanked for providing the facilities for conducting the functional assays. We acknowledge the Innovation Fund Denmark for cofinancing Ph.D. stipends to E.M.B., P.K.W, and S.B.v.W.

■ ABBREVIATIONS USED

ANOVA, analysis of variance; *t*BuOH, *tert*-butanol; DIC, *N*,*N*′-diisopropylcarbodiimide; diflunisal-desfluoro, 4-hydroxy-[1,1′-biphenyl]-3-carboxylic acid; DIPEA, *N*,*N*-diisopropylethylamine; DLS, dynamic light scattering; DMEM, Dulbecco's Modified Eagle Medium; EDC, 1-ethyl-3-(3-(dimethylamino)-propyl)carbodiimide; EtOAc, ethyl acetate; ESI-MS, electrospray ionization mass spectrometry; Fmoc-O2Oc-OH, Fmoc-8-amino-3,6-dioxaoctanoic acid; GLP-1, glucagon-like peptide 1; HATU, *N*-[(1*H*-azabenzotriazol-1-yl)(dimethylamino)-methylene]-*N*-methylmethanaminium hexafluorophosphate *N*-oxide; HBSS, Hank's Balanced Salt Solution; HBTU, *N*-[(1*H*-benzotriazol-1-yl)(dimethylamino)methylene]-*N*-methylmethanaminium hexafluorophosphate *N*-oxide; HEPES, 4-(2-hydroxyethyl)-1-piperazineethanesulfonic acid; HM-2, HerdsMan-2; NHS, *N*-hydroxysuccinimide; HOAt, 1-hydroxy-7-azabenzotriazol; MeIm, 1-methylimidazole; OGTT, oral glucose tolerance test; RU, response unit; SEC, size exclusion chromatography; SPR, surface plasmon resonance; SPPS, solid-phase peptide synthesis; SLS, static light scattering; TES, triethylsilane; $Pd(OH)_2/C$, palladium hydroxide on carbon; V_R, retention volume

DOI: 10.1021/acs.jmedchem.7b00787
J. Med. Chem. 2017, 60, 7434−7446

REFERENCES

(1) Fasano, M.; Curry, S.; Terreno, E.; Galliano, M.; Fanali, G.; Narciso, P.; Notari, S.; Ascenzi, P. The Extraordinary Ligand Binding Properties of Human Serum Albumin. *IUBMB Life* **2005**, *57* (12), 787−796.

(2) *Victoza (Liraglutide) EPAR Assessment Report*; European Medicines Agency: London, 2009; http://www.ema.europa.eu/docs/en_GB/document_library/EPAR_-_Public_assessment_report/human/001026/WC500050016.pdf (accessed Mar 1, 2017).

(3) Agersø, H.; Jensen, L. B.; Elbrønd, B.; Rolan, P.; Zdravkovic, M. The Pharmacokinetics, Pharmacodynamics, Safety and Tolerability of NN2211, a New Long-Acting GLP-1 Derivative, in Healthy Men. *Diabetologia* **2002**, *45*, 195−202.

(4) Sleep, D.; Cameron, J.; Evans, L. R. Albumin as a Versatile Platform for Drug Half-Life Extension. *Biochim. Biophys. Acta, Gen. Subj.* **2013**, *1830*, 5526−5534.

(5) Ghuman, J.; Zunszain, P. A.; Petitpas, I.; Bhattacharya, A. A.; Otagiri, M.; Curry, S. Structural Basis of the Drug-Binding Specificity of Human Serum Albumin. *J. Mol. Biol.* **2005**, *353*, 38−52.

(6) Mao, H.; Hajduk, P. J.; Craig, R.; Bell, R.; Borre, T.; Fesik, S. W. Rational Design of Diflunisal Analogues with Reduced Affinity for Human Serum Albumin. *J. Am. Chem. Soc.* **2001**, *123* (5), 10429−10435.

(7) Vallianatou, T.; Lambrinidis, G.; Tsantili-Kakoulidou, A. In Silico Prediction of Human Serum Albumin Binding for Drug Leads. *Expert Opin. Drug Discovery* **2013**, *8* (5), 583−595.

(8) Hall, M. L.; Jorgensen, W. L.; Whitehead, L. Automated Ligand- and Structure-Based Protocol for in Silico Prediction of Human Serum Albumin Binding. *J. Chem. Inf. Model.* **2013**, *53* (4), 907−922.

(9) Zhivkova, Z.; Doytchinova, I. Quantitative Structure—Plasma Protein Binding Relationships of Acidic Drugs. *J. Pharm. Sci.* **2012**, *101* (12), 4627−4641.

(10) Koehler, M. F. T.; Zobel, K.; Beresini, M. H.; Caris, L. D.; Combs, D.; Paasch, B. D.; Lazarus, R. a. Albumin Affinity Tags Increase Peptide Half-Life in Vivo. *Bioorg. Med. Chem. Lett.* **2002**, *12* (20), 2883−2886.

(11) Zobel, K.; Koehler, M. F. T.; Beresini, M. H.; Caris, L. D.; Combs, D. Phosphate Ester Serum Albumin Affinity Tags Greatly Improve Peptide Half-Life in Vivo. *Bioorg. Med. Chem. Lett.* **2003**, *13* (9), 1513−1515.

(12) Han, J.; Sun, L.; Chu, Y.; Li, Z.; Huang, D.; Zhu, X.; Qian, H.; Huang, W. Design, Synthesis, and Biological Activity of Novel Dicoumarol Glucagon-like Peptide 1 Conjugates. *J. Med. Chem.* **2013**, *56* (24), 9955−9968.

(13) Dumelin, C. E.; Trüssel, S.; Buller, F.; Trachsel, E.; Bootz, F.; Zhang, Y.; Mannocci, L.; Beck, S. C.; Drumea-Mirancea, M.; Seeliger, M. W.; Baltes, C.; Müggler, T.; Kranz, F.; Rudin, M.; Melkko, S.; Scheuermann, J.; Neri, D. A Portable Albumin Binder from a DNA-Encoded Chemical Library. *Angew. Chem., Int. Ed.* **2008**, *47* (17), 3196−3201.

(14) Sun, L.; Wang, C.; Dai, Y.; Chu, Y.; Han, J.; Zhou, J.; Cai, X.; Huang, W.; Qian, H. Coumaglutide, a Novel Long-Acting GLP-1 Analog, Inhibits β-Cell Apoptosis in Vitro and Invokes Sustained Glycemic Control in Vivo. *Eur. J. Pharmacol.* **2015**, *767*, 211−219.

(15) Brabez, N.; Saunders, K.; Nguyen, K. L.; Jayasundera, T.; Weber, C.; Lynch, R. M.; Chassaing, G.; Lavielle, S.; Hruby, V. J. Multivalent Interactions: Synthesis and Evaluation of Melanotropin Multimers - Tools for Melanoma Targeting. *ACS Med. Chem. Lett.* **2013**, *4* (1), 98−102.

(16) Knudsen, L. B.; Nielsen, P. F.; Huusfeldt, P. O.; Johansen, N. L.; Madsen, K.; Pedersen, F. Z.; Thøgersen, H.; Wilken, M.; Agersø, H. Potent Derivatives of Glucagon-like Peptide-1 with Pharmacokinetic Properties Suitable for Once Daily Administration. *J. Med. Chem.* **2000**, *43* (9), 1664−1669.

(17) Finan, B.; Yang, B.; Ottaway, N.; Stemmer, K.; Müller, T. D.; Yi, C.-X.; Habegger, K.; Schriever, S. C.; García-Cáceres, C.; Kabra, D. G.; Hembree, J.; Holland, J.; Raver, C.; Seeley, R. J.; Hans, W.; Irmler, M.; Beckers, J.; de Angelis, M. H.; Tiano, J. P.; Mauvais-Jarvis, F.; Perez-Tilve, D.; Pfluger, P.; Zhang, L.; Gelfanov, V.; DiMarchi, R. D.; Tschöp, M. H. Supplementary Information, Targeted Estrogen Delivery Reverses the Metabolic Syndrome. *Nat. Med.* **2012**, *18* (12), 1847−1856.

(18) Sudlow, G.; Birkett, D. J.; Wade, D. N. The Characterization of Two Specific Drug Binding Sites on Human Serum Albumin. *Mol. Pharmacol.* **1975**, *11*, 824−832.

(19) Sudlow, G.; Birkett, D. J.; Wade, D. N. Further Characterization of Specific Drug Binding Sites on Human Serum Albumin. *Mol. Pharmacol.* **1976**, *12*, 1052−1061.

(20) Kragh-Hansen, U.; Chuang, V. T. G.; Otagiri, M. Practical Aspects of the Ligand-Binding and Enzymatic Properties of Human Serum Albumin. *Biol. Pharm. Bull.* **2002**, *25* (June), 695−704.

(21) Yang, F.; Yue, J.; Ma, L.; Ma, Z.; Li, M.; Wu, X.; Liang, H. Interactive Associations of Drug-Drug and Drug-Drug-Drug with Iia Subdomain of Human Serum Albumin. *Mol. Pharmaceutics* **2012**, *9* (11), 3259−3265.

(22) Hüll, M.; Lieb, K.; Fiebich, B. L. Anti-Inflammatory Drugs: A Hope for Alzheimer's Disease? *Expert Opin. Invest. Drugs* **2000**, *9* (4), 671−683.

(23) Haworth, R.; Oakley, K.; McCormack, N.; Pilling, A. Differential Expression of COX-1 and COX-2 in the Gastrointestinal Tract of the Rat. *Toxicol. Pathol.* **2005**, *33*, 239−245.

(24) Finan, B.; Yang, B.; Ottaway, N.; Stemmer, K.; Müller, T. D.; Yi, C.-X.; Habegger, K.; Schriever, S. C.; García-Cáceres, C.; Kabra, D. G.; Hembree, J.; Holland, J.; Raver, C.; Seeley, R. J.; Hans, W.; Irmler, M.; Beckers, J.; de Angelis, M. H.; Tiano, J. P.; Mauvais-Jarvis, F.; Perez-Tilve, D.; Pfluger, P.; Zhang, L.; Gelfanov, V.; DiMarchi, R. D.; Tschöp, M. H. Targeted Estrogen Delivery Reverses the Metabolic Syndrome. *Nat. Med.* **2012**, *18* (12), 1847−1856.

(25) *Victoza (Liraglutide) Full Prescription Information*; Nordisk Novo A/S: Bagsvaerd, Denmark, 2010; https://www.accessdata.fda.gov/drugsatfda_docs/label/2010/022341lbl.pdf (accessed Feb 22, 2017).

(26) *Indocin (Indomethacin) Oral Suspension*; IROKO Pharmaceuticals, LLC: Philadelphia, 2008; https://www.accessdata.fda.gov/drugsatfda_docs/label/2009/018332s032lbl.pdf (accessed Jan 22, 2017).

(27) *Dolobid (Diflunisal) Tablets*; Merck & Co. Inc.: Whitehouse Station, NJ, 2007; www.accessdata.fda.gov/drugsatfda_docs/2007/018445s058lbl.pdf (accessed Feb 22, 2017).

(28) Laue, T.; Plagens, A. Williamson Ether Synthesis. In *Named Organic Reactions*; John Wiley and Sons, Ltd: Chichester, UK, 2005; pp 19−49.

(29) Steensgaard, D. B.; Thomsen, J. K.; Olsen, H. B.; Knudsen, L. B. The Molecular Basis for the Delayed Absorption of the Once-Daily Human GLP-1 Analog, Liraglutide. In *Diabetes: American Diabetes Association's (ADA) 68th Scientific Sessions, San Francisco, 2008*, 2008; Vol. *57*, p A157.

(30) Rich, R. L.; Myszka, D. G. Grading the Commercial Optical Biosensor Literature-Class of 2008: "The Mighty Binders. *J. Mol. Recognit.* **2010**, *23* (1), 1−64.

(31) Jonassen, I.; Havelund, S.; Hoeg-Jensen, T.; Steensgaard, D. B.; Wahlund, P. O.; Ribel, U. Design of the Novel Protraction Mechanism of Insulin Degludec, an Ultra-Long-Acting Basal Insulin. *Pharm. Res.* **2012**, *29* (8), 2104−2114.

(32) Younis, N.; Soran, H.; Bowen-Jones, D. Insulin Glargine: A New Basal Insulin Analogue. *Ann. Pharmacother.* **2002**, *36*, 1019−1027.

(33) Madsen, K.; Knudsen, L. B.; Agersoe, H.; Nielsen, P. F.; Thøgersen, H.; Wilken, M.; Johansen, N. L. Structure-Activity and Protraction Relationship of Long-Acting Glucagon-like Peptide-1 Derivatives: Importance of Fatty Acid Length, Polarity, and Bulkiness. *J. Med. Chem.* **2007**, *50* (24), 6126−6132.

(34) Lau, J.; Bloch, P.; Schäffer, L.; Pettersson, I.; Spetzler, J.; Kofoed, J.; Madsen, K.; Knudsen, L. B.; McGuire, J.; Steensgaard, D. B.; Strauss, H. M.; Gram, D. X.; Knudsen, S. M.; Nielsen, F. S.; Thygesen, P.; Reedtz-Runge, S.; Kruse, T. Discovery of the Once-Weekly Glucagon-Like Peptide-1 (GLP-1) Analogue Semaglutide. *J. Med. Chem.* **2015**, *58* (18), 7370−7380.

DOI: 10.1021/acs.jmedchem.7b00787
J. Med. Chem. 2017, 60, 7434−7446

(35) Russell-Jones, D. Molecular, Pharmacological and Clinical Aspects of Liraglutide, a Once-Daily Human GLP-1 Analogue. *Mol. Cell. Endocrinol.* **2009**, *297*, 137−140.
(36) Deryabina, M. A.; Daugaard, J. R.; Knudsen, C. B.; Shelton, P. T.; Fog, J. U.; Jessen, L.; Noerregaard, P. Pharmacokinetics and Pharmacodynamics of GLP-1-GIP Receptor Dual Agonist Peptides: From Once-Daily to Once-Weekly. In *Integrated Physiology - Other Hormones: The American Diabetes Association's (ADA) 75th Scientific Sessions, Boston, 2015*, 2015; p 2086-P.
(37) Tofteng Shelton, P.; J. Jensen, K. Linkers, Resins, and General Procedures for Solid-Phase Peptide Synthesis. In *Peptide Synthesis and Applications*; J. Jensen, K.; Tofteng Shelton, P.; L. Pedersen, S., Eds.; Humana Press: Totowa, NJ, 2013; pp 23−43.
(38) Mathiesen, J. M.; Vedel, L.; Bräuner-Osborne, H. cAMP Biosensors Applied in Molecular Pharmacological Studies of G Protein-Coupled Receptors. In *Methods Enzymol.*. Pyle, A. M., Christianson, D. W., Eds.; Elsevier: New York, 2013; Vol. *522*, pp 191−207.
(39) Rich, R. L.; Day, Y. S.; Morton, T. A.; Myszka, D. G. High-Resolution and High-Throughput Protocols for Measuring Drug/human Serum Albumin Interactions Using BIACORE. *Anal. Biochem.* **2001**, *296*, 197−207.

■ NOTE ADDED AFTER ASAP PUBLICATION

After this paper was published ASAP on August 16, 2017, a correction was made to the name of author Manuel C. Martos-Maldonado. The corrected version was reposted August 25, 2017.

DOI: 10.1021/acs.jmedchem.7b00787
J. Med. Chem. 2017, 60, 7434−7446